State of New Jersey

DEPARTMENT OF ENVIRONMENTAL PROTECTION

CHRIS CHRISTIE
Governor

KIM GUADAGNO
Lt. Governor

Water Resource Management
New Jersey Geological Survey
Mail Code: 29-01
29 Arctic Pkwy
PO Box 420
Trenton, NJ 08625-0420
Tel. # (609) 292-1185 – Fax (609) 633-1004 – Home Page: http//www.njgeology.org/

BOB MARTIN
Commissioner

TO: Joe Marchesani, SRP – Ground Water Pollution Abatement

THROUGH: John Curran, Section Chief, Geoscience Research and Support Section, BWR, NJGS
Dave Pasiczynk, Chief, Bureau of Water Resources, NJ Geological Survey
Karl Muessig, State Geologist, NJ Geological Survey, Water Resource Management, DEP

FROM: Gregory Herman, Research Scientist 1, NJDEP-WRM-NJGS-BWR-GRASS

RE: Interpretation of Borehole Televiewer Data and hydrogeological framework for the Picatinny Arsenal Mid-Valley groundwater investigation

The NJGS received a request for geological support from the NJDEP-Site Remediation Program on March 23, 2010 for conducting a structural analysis of borehole televiewer (BTV) data in support of project work on the Picatinny Arsenal Mid-Valley groundwater pollution site. Shortly afterwards, interpreted acoustic televiewer records were made available to the NJGS for three monitoring wells (MW6C, MW-10B, and MW-11) drilled into Precambrian crystalline bedrock (figs. 1 and 2). The records were recorded and interpreted by Mid-Atlantic Geosciences, a division of Enviroscan, Inc., under contract by Arcadis, the environmental consulting firm hired by the US Army to conduct the groundwater characterization and remediation of the Mid-Valley site. The NJGS conducted a structural analysis of these data (fig. 3) that was forwarded to Mr. Marchesani in late April for distribution to the responsible parties and their representatives. A second request for a structural geological analysis of new BTV data for a fourth monitoring well at the site (MW-11B, figs. 1 and 2) was received by the NJGS from Mr. Marchesani on February 25, 2011. The new data included both acoustic televiewer (ATV) and optical televiewer (OPTV) records. The new OPTV record was also generated and interpreted by Mid-Atlantic Geosciences.

The interpretation of the first three wells with ATV records was limited to conducting rose diagram and stereonet structural analyses of the fractures logged and interpreted by Mid-Atlantic Geosciences (fig. 3). The ATV records are generated using measurements and displays of travel-times and amplitude variations of sound waves that that are emitted by an acoustic source and reflected off the borehole wall back to an acoustic receiver. Incremental variations in these parameters provide a record of the physical variations in the rock including cavities, matrix density changes, and structural discontinuities such as faults and fractures. OPTV records are produced using reflected light and are therefore a photographic record of the borehole and the penetrated structural features. The BTV records include incremental magnetometer and inclinometer data embedded in the digital data with the resulting images showing structural data with three dimensional orientations in the subsurface. The OPTV produces a record of the rock color and textures that are necessary to conduct a more thorough geological interpretation of the bedrock features, and a basis for discriminating between primary geological structures including bedding, foliation, or layering from secondary structural features such as cleavage, fractures, folds, and faults. ATV records are also useful in boreholes with turbid water and in drilling operations requiring muddy drilling fluids so that porous borehole features can be imaged through an obscuring medium. However, in water wells that are dry or with relatively clear water, OPTV data are preferred as a geological mapping tool as they provide a basis for discriminating between the primary and secondary structures. Ideally, boreholes having both ATV and OPTV records provide the best results for the identifying and interpreting subsurface geological features that store and transmit groundwater. Because the new well (MW-11B) has both ATV

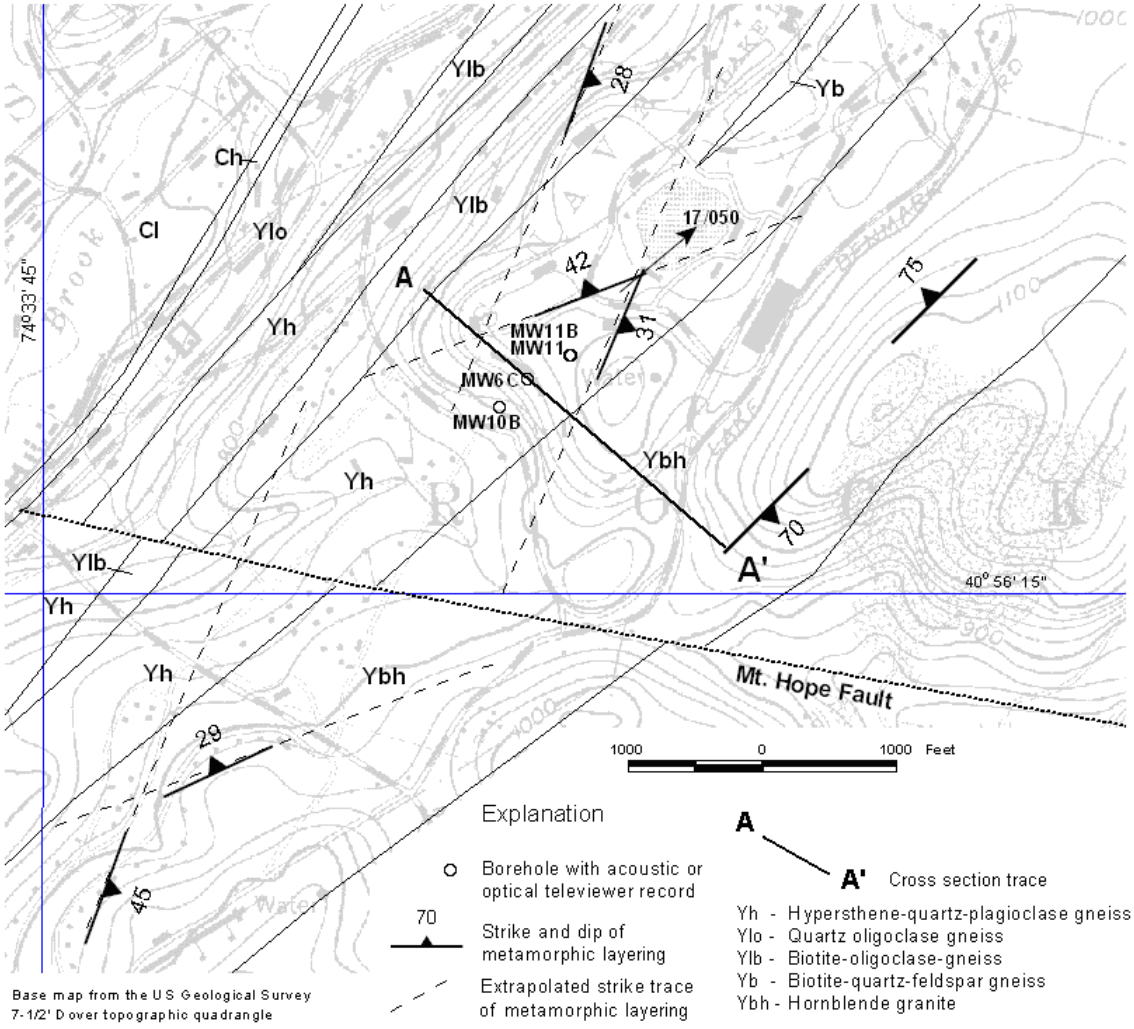

Figure 1. Geological map of the Mid-Valley Groundwater Pollution site modified from an unpublished compilation of the bedrock geology of the Dover 7-1/2' quadrangle by Rich Volkert, NJ Geological Survey, showing the location of four monitoring wells with recent borehole televiewer data.

and OPTV records, a more complete structural analysis of the borehole, and the hydrogeological setting of the site was possible.

The structural interpretation of the MW-11B borehole conducted by the NJGS was based on the interpreted record provided by Mid-Atlantic Geosciences. Their interpretation only included the orientation of fractures in the borehole walls, with designation of the fractures as being either open or sealed. I assume that these designations correspond to fractures being hydraulically conductive (open) versus nonconductive (sealed). However, the OPTV record clearly shows metamorphic layering dipping at low-to moderate angles throughout the length of the borehole (table 1 and fig. 4). A structural analysis of the orientation of metamorphic layering was conducted by visually inspecting the interpreted record and noting in table 1 where the measured fractures were parallel to the metamorphic layering, defined by the variable distribution of the different light- and dark-colored minerals in planar arrangement in the rock matrix. Orientation data for the layering was input into a computer program for circular histogram and stereonet analyses of primary structural trends (fig. 5). The structural analysis shows that the metamorphic layers are folded into a series of open, upright folds with fold axes plunging gently northeastward (the Beta axis in fig. 5b with trend/plunge of N50E/17). The primary strikes and dips of metamorphic layering and the fold axis from figure 5 are plotted on figure 1. Reviewing the tabulated orientation data by depth (fig. 6) shows that well MW-11B contains panels of layered gneiss and foliated granite dipping alternating from

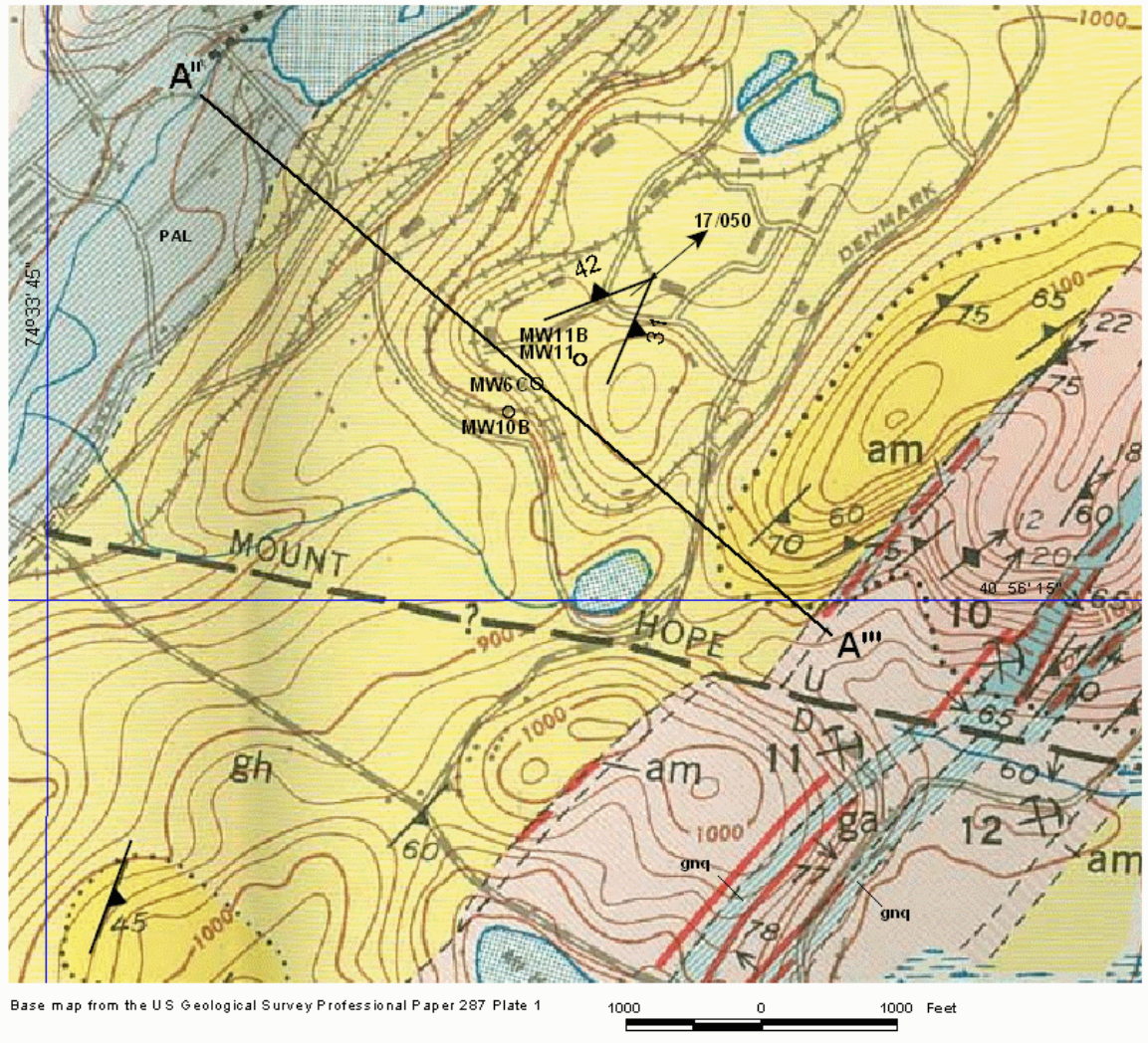

Figure 2. Regional geological map odf the Dover magnetite district in the vicinity of the Mid-Valley groundwater pollution site from Simms and Buddington (1958).

moderately NW to gently SE (table 1). The relative abundance of NW dips is about twice as for the SE dips (fig. 5). These results were used to construct the cross section interpretation (fig. 7). The strike of primary foliation determined from the OPTV survey are parallel to the outcrop measurements, and are emphasized in figure 1 using dashed lines drawn through the strikes. Figure 1 also shows that bedrock foliation dips steeper to the southeast and gentler to the northwest. Outcrops in the area are relatively scarce as the area lies within glaciated terrain with abundant surficial deposits that locally cover bedrock.

The cross section (fig. 7) depicts crinkled and folded metamorphic layers dipping moderately northwest approaching the Paleozoic valley to the northwest and more steeply progressing across the area to the southeast. This interpretation differs from those depicted in the Arcadis (February 2011 presentation (page 9), and in the Sims and Buddington (1958) interpretation, that both depict metamorphic layers dipping steeply SE throughout the region. However, both the OPTV record and the core photographs included in the Arcadis (Februrary 2011) report (pages 12, 13 and 18) reveal gentle-to-moderate-dipping layers beneath the site.

The geological units underlying the site are interpreted differently by Simms and Buddington (fig. 2) and Volkert (fig. 1). Figure 2 shows the site underlain and surrounded by gneissoid hornblende granite (gh) whereas figure 1 shows the site underlain by layered metamorphic rocks with hornblende granite (Ybh) to the southeast (fig,. 6). I didn't inspect the cores from the site, but an inspection of the OPTV

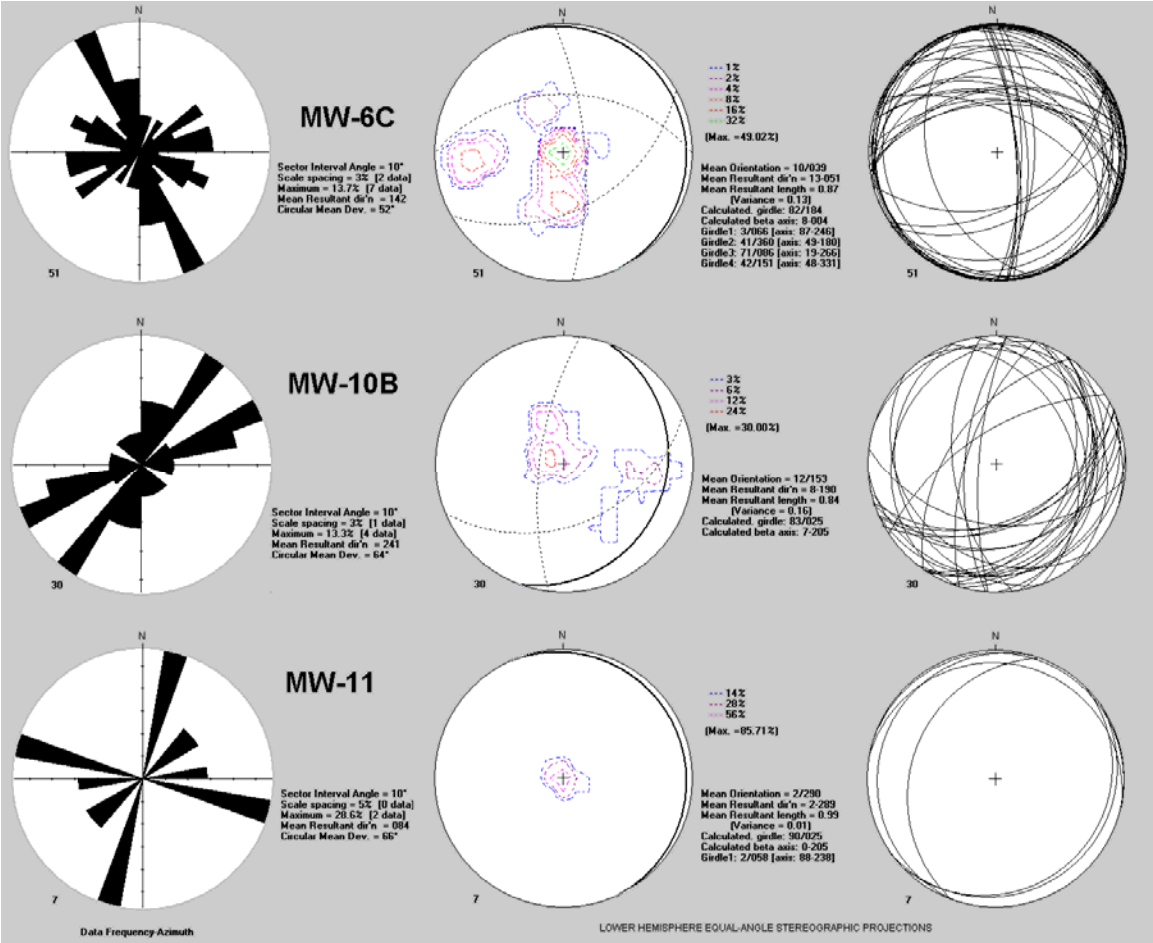

Figure 3. Structural analyses of interpreted ATV records collected during the first phase of the BTV studies showing the orientation of fractures in three bedrock wells.

record suggests that well MW-11B penetrated both layered metamorphic rocks and foliated gneissoid granite, and therefore is more in line with the mapping shown in figure 1.

To conclude, there are four other points of interest to consider:

1) Most of the hydraulically conductive (open) fractures noted in the OPTV record for well MW-11B follow metamorphic layering, and are probably secondary pores that are open within the fold hinges of the crinkled bedrock layers. This probably reflects fold-hinge porosity, with the pores plunging gently northeastward along the local fold axes.

2). The rusty-colored staining that occurs along most of the open fractures may indicate zones of contaminated groundwater flow, as was inferred from OPTV records in other VOC groundwater contamination sites underlain by Precambrian rocks in the NJ Highlands (Herman, 2006). Rusty-colored staining of the matrix along a fracture wall in core (Arcadis, February 2011, page 18) is noted as matrix alteration. However, the matrix of the Precambrian silicate crystalline rocks is generally impervious in the absence of brittle fracturing, and the staining near the fracture walls is a result of secondary porosity and permeability imparted by fracturing at the microscopic scale adjacent to the visible fracture surfaces. Each fracture seen in the BTV records and core is the visible part of a larger volume of rock locally including a range of microscopic to macroscopic fractures operating within a 'fracture process zone'. Ordinarily, the visible fracture occupies the central part of the process zone where coalescence and linkage of smaller fractures results in a larger plane of structural discontinuity.

3) The areas of the contaminant plume depicted in the map (Arcadis, February 2011, fig. 16) and subsurface (Arcadis, February 2011, fig. 17) do not agree. The map shows the plume limits for the 10 ug/L isopleth are southwest of the MW-11 well cluster, but extends beyond this same well cluster in the profile

view. It is interesting to note that the upper surface of the plume that is inclined to the northeast (from left to right in Arcadis, February 2011, fig. 17) in inclined at a shallow angle similar to the plunge of the fold-axis determined from the structural analysis of OPTV data (fig. 5). Therefore, the plume distribution follows downward topographic gradients to the west, but gently-plunging structural fold axes to the northeast. It is possible that the plume extends beyond the MW-11 cluster in the subsurface along the N50^{o}E fold trend noted above. Well MW-12, having no detectable VOCs may be located to far to the southeast to have intersected the plume in the more northeastward reaches of the area.

4). The horizontal and vertical extent of the plume may be different than currently defined in the Arcadis presentation. The horizontal extent has been mistakenly represented in comparison to the profile depiction of the plume extent, and all of the wells defining the plume terminate within the plume. It would be interesting to explore observed contaminant concentration gradients in both the horizontal and vertical dimension using known control points in an attempt to better quantify the physical dimensions of the plume, particularly in the area of the MW-11 well cluster.

References

Arcadis, February 2011, Updated groudnwater model, Mid-Valley groundwater (PICA 2004), 52 p.

Herman, G. C., 2006, Hydrogeological framework of Middle Proterozoic granite and gneiss from borehole geophysical surveys at two ground-water pollution sites, Morris County, NJ: *in* Macaoay, Suzanne, and Montgomery, William, Editors, Environmental Geology of the Highlands, 23rd Annual Meeting of the Geological Association of New Jersey, Ramapo College of New Jersey, Mahwah, New Jersey, p. 26-45.

N.J. Geological Survey, 2001, Arcview 3.X Extension for Well-field generation and visualization, Digital Geodata Series DGS01-1. Unpublished modifications to a computer software extension to provide support for borehole televiewer data.

Sims, P.K., and Buddington, A.F., 1958, Geology and magnetite deposits of Dover district, Morris County, New Jersey: U.S. Geological Survey Professional Paper 287, 162 p.

Table 1. Summary of Optical Televiewer fracture data for well MW-11B and layering interpretation.

ID	DEPTH	BRG	INC	DD	C1	C2	C3
1	25	356	84	west	Open	Fracture	
2	25.7	352	46	west	Open	Fracture	Layering
3	30.3	342	63	west	Open	Fracture	
4	31.9	329	41	west	Sealed	Fracture	Layering
5	43.4	7	58		Open	Fracture	
6	45.9	343	62	west	Open	Fracture	Layering
7	46.4	346	57	west	Sealed	Fracture	Layering
8	46.5	346	58	west	Sealed	Fracture	Layering
9	47.2	347	53	west	Sealed	Fracture	Layering
10	50.7	320	84	west	Open	Fracture	
11	53.2	335	38	west	Sealed	Fracture	Layering
12	56.4	18	32		Open	Fracture	Layering
13	57.5	344	46	west	Sealed	Fracture	Layering
14	58.1	301	47	west	Sealed	Fracture	
15	58.6	334	40	west	Sealed	Fracture	Layering
16	60.8	22	34	east	Sealed	Fracture	
17	70.5	135	29	east	Sealed	Fracture	
18	71.3	309	53	west	Open	Fracture	Layering
19	71.5	307	30	west	Open	Fracture	
20	71.9	299	26	west	Open	Fracture	
21	76.8	321	28	west	Open	Fracture	
22	85.8	231	18	west	Sealed	Fracture	

23	86.3	325	59	west	Sealed	Fracture	
24	86.6	132	27	east	Open	Fracture	Layering
25	87.5	129	56	east	Sealed	Fracture	Layering
26	88.5	157	16	east	Open	Fracture	
27	88.6	147	14	east	Open	Fracture	
28	91	329	74	west	Open	Fracture	
29	91.7	342	37	west	Open	Fracture	
30	92.3	333	67	west	Open	Fracture	
31	92.7	339	61	west	Sealed	Fracture	
32	92.8	346	59	west	Sealed	Fracture	
33	94	344	62	west	Open	Fracture	
34	94.7	341	66	west	Open	Fracture	
35	97.9	347	74	west	Open	Fracture	
36	101	340	72	west	Open	Fracture	
37	108.1	114	51	east	Sealed	Fracture	Layering
38	109.4	115	33	east	Open	Fracture	Layering
39	114.2	41	2	east	Open	Fracture	
40	115.7	303	21	west	Open	Fracture	
41	116.5	330	35	west	Sealed	Fracture	
42	118.3	0	46		Open	Fracture	
43	119.4	105	8	east	Open	Fracture	
44	121.8	179	46	east	Sealed	Fracture	
45	122.6	35	18	east	Sealed	Fracture	
46	122.9	355	58	east	Open	Fracture	Layering
47	131.1	167	36	east	Sealed	Fracture	
48	133.7	318	46	west	Zone	Fracture	Layering
49	135.7	305	34	west	Open	Fracture	
50	136.1	288	37	west	Open	Fracture	
51	136.8	329	43	west	Open	Fracture	Layering
52	137.5	354	40	west	Open	Fracture	Layering
53	138.7	318	40	west	Open	Fracture	Layering
54	139.1	323	61	west	Open	Fracture	Contact
55	139.3	176	11		Sealed	Fracture	
56	140.8	334	61	west	Sealed	Fracture	
57	152.2	134	27		Open	Fracture	
58	152.7	291	32		Open	Fracture	
59	154.7	328	9	west	Open	Fracture	
60	156	335	15	west	Open	Fracture	
61	160.4	89	31	east	Sealed	Fracture	Layering
62	160.6	96	34	east	Sealed	Fracture	Layering
63	161.4	205	38		Open	Fracture	
64	168.7	102	27	east	Sealed	Fracture	Layering
65	170.5	313	27	west	Sealed	Fracture	
66	173.1	333	27	west	Sealed	Fracture	
67	178.4	137	56		Sealed	Fracture	
68	178.8	148	37	east	Open	Fracture	
69	179.4	95	77	east	Open	Fracture	
70	181.5	111	49	east	Open	Fracture	
71	184.5	126	32	east	Open	Fracture	Layering
72	184.8	133	16	east	Open	Fracture	
73	189.9	304	32	east	Sealed	Fracture	Layering
74	190.7	283	36		Open	Fracture	
75	192.1	122	12	east	Open	Fracture	
76	192.6	83	76	east	Sealed	Fracture	
77	192.9	323	38	west	Sealed	Fracture	
78	194.4	68	69		Open	Fracture	
79	200.2	337	42	west	Open	Fracture	Layering

Note: BRG – bearing, INC – inclination (dip), DD – dip direction, C1 to C3 are fracture attributes.

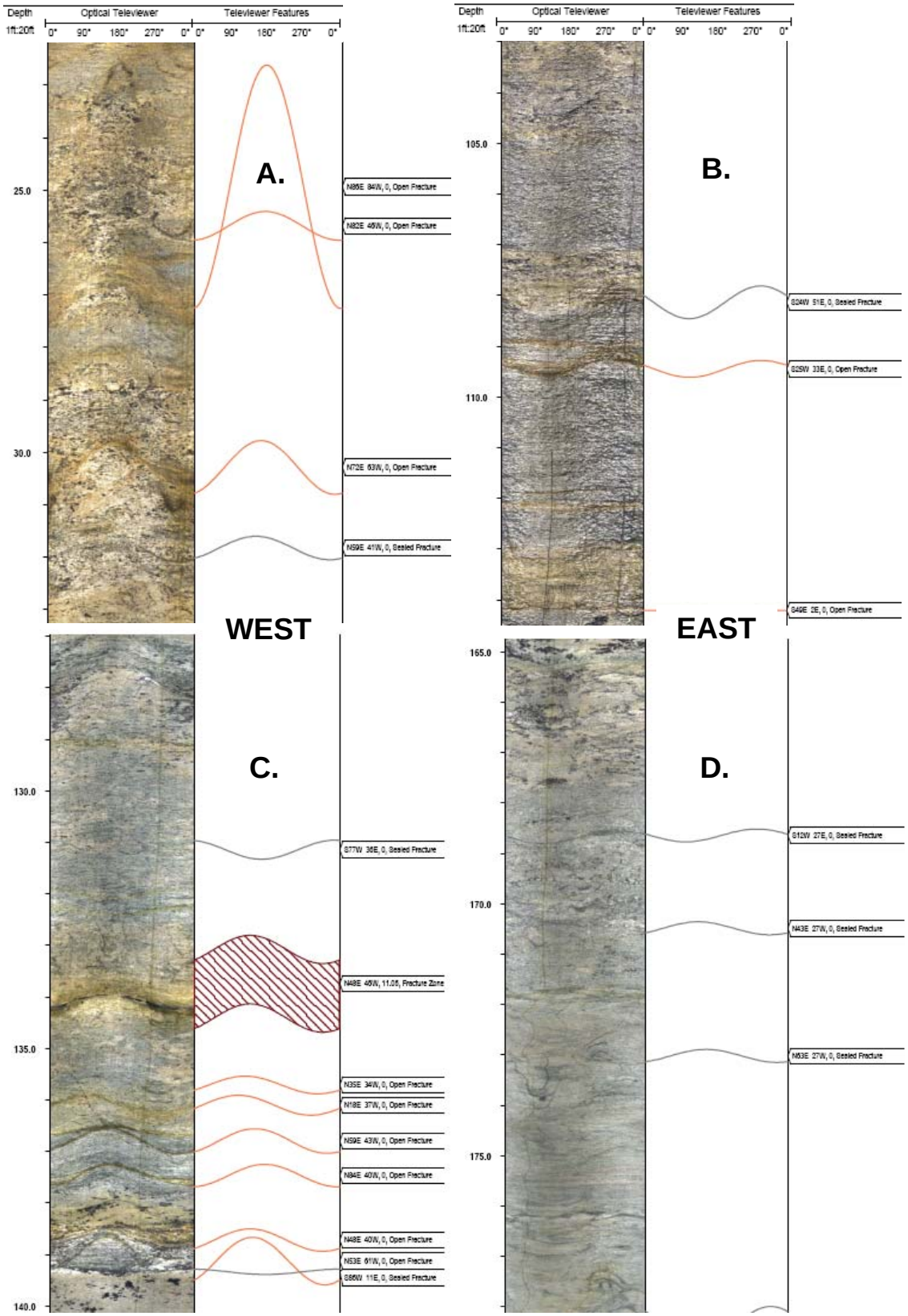

Figure 4. Interpreted OPTV records for well MW-llB showing open and sealed fractures formed along metamorphic layering dipping at gentle-to-moderate angles to the west (4A and 4C) and east (4B and 4D).

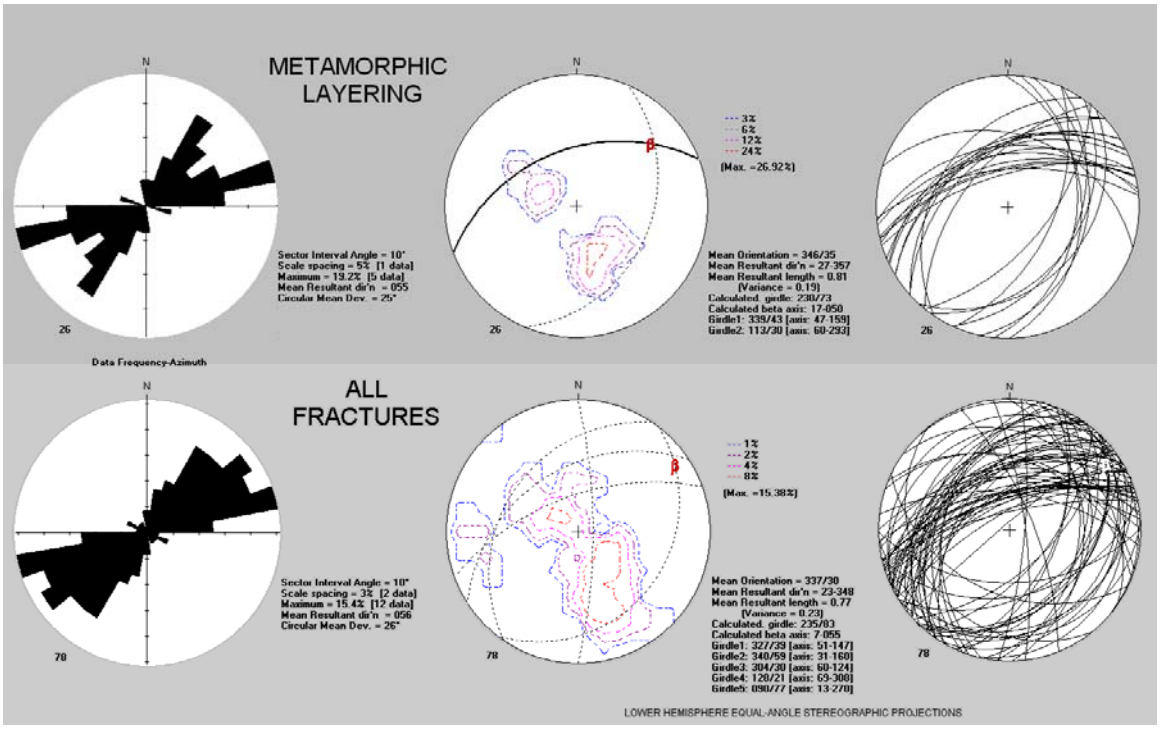

Figure 5. Structural analyses of interpreted OPTV records for well MW-11B showing the bimodal distribution of metamorphic layering (A) and the orientation of all fractures (B).

ID	DEPTH	BRG	INC	DD	C1	C2	C3
2	25.7	352	46	west	Open	Fracture	Layering
4	31.9	329	41	west	Sealed	Fracture	Layering
6	45.9	343	62	west	Open	Fracture	Layering
7	46.4	346	57	west	Sealed	Fracture	Layering
8	46.5	346	58	west	Sealed	Fracture	Layering
9	47.2	347	53	west	Sealed	Fracture	Layering
11	53.2	335	38	west	Sealed	Fracture	Layering
12	56.4	18	32		Open	Fracture	Layering
13	57.5	344	46	west	Sealed	Fracture	Layering
15	58.6	334	40	west	Sealed	Fracture	Layering
18	71.3	309	53	west	Open	Fracture	Layering
24	86.6	132	27	east	Open	Fracture	Layering
25	87.5	129	56	east	Sealed	Fracture	Layering
37	108.1	114	51	east	Sealed	Fracture	Layering
38	109.4	115	33	east	Open	Fracture	Layering
46	122.9	355	58	east	Open	Fracture	Layering
48	133.7	318	46	west	Zone	Fracture	Layering
51	136.8	329	43	west	Open	Fracture	Layering
52	137.5	354	40	west	Open	Fracture	Layering
53	138.7	318	40	west	Open	Fracture	Layering
54	139.1	323	61	west	Open	Fracture	Contact
61	160.4	89	31	east	Sealed	Fracture	Layering
62	160.6	96	34	east	Sealed	Fracture	Layering
64	168.7	102	27	east	Sealed	Fracture	Layering
71	184.5	126	32	east	Open	Fracture	Layering
73	189.9	304	32	east	Sealed	Fracture	Layering
79	200.2	337	42	west	Open	Fracture	Layering

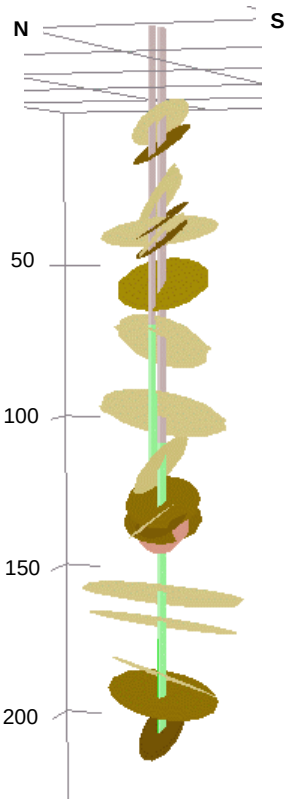

Figure 6. List and plot of layering dip direction (DD) in the borehole. Layers are plotted in the vertical dimension (right) using ArcView 3D Analyst and a custom program by the NJ Geological Survey (2001)

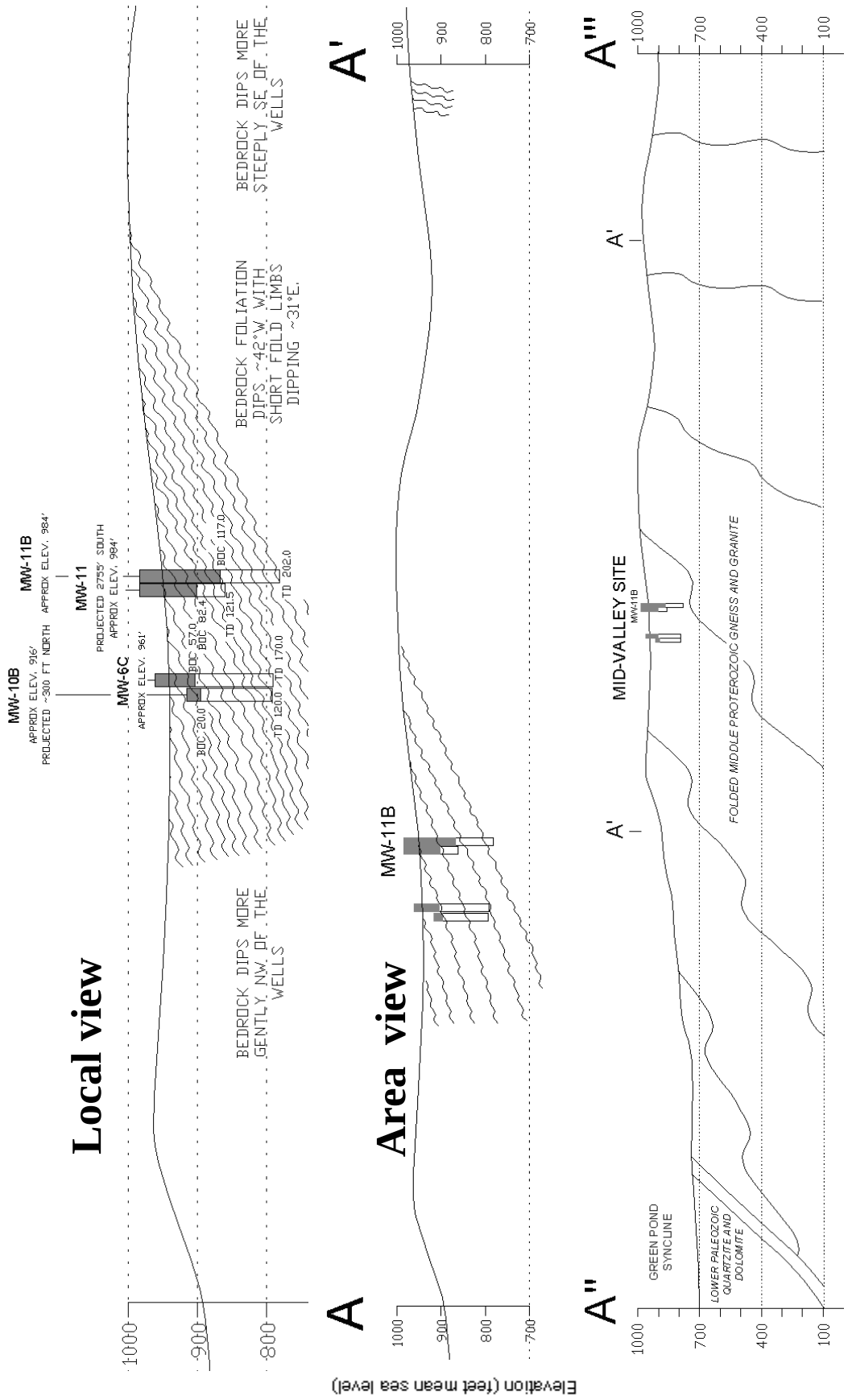

Figure 7. Local, area, and regional Cross section views of the Mid-Valley pollution site. Cross section detail decreases from top to bottom. The profile traces for the lower two sections are shown on figure 1 and 2 respectively.